ISSN 2706-655X Vol.6, Issue 6: 8-17, DOI: 10.25236/IJFET.2024.060602

Numerical Simulation of Passive Q-switched Solid-state Laser Based on Graphene

Danqing Long[a,*], Tianlong Bai[b]

Hunan University of Science and Technology, Xiangtan, China
[a]18773906864@163.com, [b]15128910694@163.com
[*]Corresponding author

Abstract: *Passively Q-switched solid-state lasers offer several advantages, including a compact structure, stable output performance, and high monochromaticity. Consequently, they are extensively employed in a wide range of applications, including industrial manufacturing, scientific research, biomedical fields, and national defense technologies. However, the use of two-dimensional materials, such as graphene, as saturable absorbers in solid-state lasers to achieve Q-switched output has been shown to exhibit decreased stability.In this study, the nonlinear optical characteristics of graphene are incorporated into the simulation model, and the Q-switched rate equations based on a four-level energy system are numerically solved using the fourth-order Runge-Kutta method. This approach successfully generates a stable Q-switched pulse sequence. Furthermore, this paper examines how variations in key system parameters, such as pump rate and intracavity losses, influence pulse width in passively Q-switched lasers. It also explores the dynamic behavior of crucial parameters, including photon number density, inversion particle number, and ground state particle number, thereby revealing insights into the laser's operational dynamics.*

Keywords: *Passively Q-switched solid-state lasers, Nonlinear optical characteristics, Saturable absorber*

1. Introduction

Solid-state lasers have become a pivotal technology in numerous industries, largely due to their compact structure, diminutive size, considerable output energy, elevated peak power, and adjustable wavelength. They have demonstrated considerable potential for application across a diverse array of sectors, including industry, military, medicine, and beyond.[1]In the industrial field, solid-state lasers are employed for precision laser cutting and welding, offering high efficiency and high precision.[2-3]In the military field, the characteristics of solid-state lasers contribute to improvements in the performance of weapon systems, particularly in distance measurement, missile navigation and positioning, as well as air defense. Furthermore, solid-state lasers are utilized in missile interception technology in long-range combat.[4]The medical field benefits from the high monochromaticity, high collimation, and energy tunability of solid-state lasers, which have become a ubiquitous tool in precision medical fields such as laser surgery, plastic surgery, and dental care.[5-6]At present, mode-locked lasers and Q-switched lasers represent the most mature laser technologies. Locking mode lasers are capable of generating ultra-short pulse lasers, with the potential to output picosecond or even femtosecond laser pulses. Q-switched lasers, meanwhile, release high peak power pulses by adjusting cavity losses, rendering them suitable for applications that require high peak power, such as laser marking, precision cutting, and medical surgery.[7-9]

Active Q-switching and passive Q-switching represent two prevalent Q-switching methodologies in laser technology. The primary distinction between these approaches pertains to the manner of regulating resonant cavity losses. Active Q-switching lasers employ external devices, such as acousto-optic or electro-optic modulators, to actively regulate the losses within the laser cavity. When the gain of the laser reaches a specific threshold, the modulator, under the control of electrical or acoustic signals, instantaneously reduces the losses within the laser cavity, thereby releasing accumulated energy and generating a high-peak pulse output.[10-11]In contrast, passive Q-switched lasers employ the introduction of saturable absorbers as passive components to automatically adjust for cavity losses. The saturable absorber exhibits a high absorption rate at low light intensity. As the light intensity increases, the absorption rate gradually decreases, resulting in a reduction in cavity loss. Following energy accumulation, the absorber releases the accumulated energy instantaneously to form a pulse output. Passive Q-switched lasers are widely used in low-cost lasers due to their simple structure and low cost.[12-13]Nevertheless, the utilisation of saturable absorbers comprising two-dimensional materials, such as graphene and black phosphorus, may present challenges in attaining a stable pulse output in solid-state lasers. This is attributed to the inherent limitations in the stability and precision of the external structure.

In 2005, Oleg A. Louchev et al. conducted numerical simulations of the dynamic and laser characteristics of a Q-switched Yb:YAG laser by solving the coupling rate equation.[14]The research team, led by Yuye Wang, employed numerical simulations to examine the influence of pump rate and pump pulse duration on the operational characteristics of passive Q-switched Nd:YAG/Cr^{4+}:YAG solid-state lasers.[15]Adrien Aubourg and colleagues employed Cr:ZnSe as a saturable absorber to develop a diode-pumped Er:YAG solid-state laser. They achieved Q-switched output at a wavelength of 1640 nm with a pulse duration of 21 ns and a pulse energy of 330 μJ.[16]Yuanyao Lin et al. used a V-shaped laser cavity configuration and a topologically insulating (TI) saturable absorber to achieve passive Q-switched pulse generation in a Nd:YAG solid-state laser operating at 1064 nm and 1340 nm wavelengths. The pulse duration was found to be 576 ns and 673 ns, with respective repetition rates of 28.57 kHz and 75.5 kHz.[17]Linjun Li et al. employed a novel WSe_2 nanosheet as a saturable absorber and Tm: YAP as a gain medium, resulting in the generation of a Q-switched output with an average output power of 1.29 W and a pulse duration of 392.7 ns at 1988.3 nm.[18]Du et al. conducted an experimental investigation into the instability of output pulses in passive QTm Ho: GdVO4 solid-state lasers, and ascribed this phenomenon to deterministic low-dimensional nonlinear dynamics.[19]Despite the aforementioned research, there is a paucity of literature on the dynamic evolution of the output characteristics of passive Q-switched solid-state lasers. Specifically, there is a lack of literature on the evolution of their Q-switched pulse width, photon number density, inverted particle number, and ground state particle number.

This article is based on the fundamental theory of the Q-switching rate equation and establishes a rate equation model for a four-level system. A numerical simulation of a passive Q-switching solid-state laser with graphene as a saturable absorber was conducted using Matlab with the adaptive step size fourth-order Runge-Kutta method. The simulation successfully yielded a stable Q-switching pulse sequence. On this basis, this article further analyses the trend of pulse width variation by changing the pumping rate of the laser pumping light source and the numerical value of the scattering loss in the laser cavity. This reveals the evolution path of photon number density, inverted particle number, and ground state particle number.

2. Theoretical Model of Passive Q-switching.

The distinction between passive Q-switched lasers and active Q-switched lasers lies in their structural simplicity and independence from external electrical or acousto-optic signals to modulate the quality factor Q value within the cavity, defined as the ratio of energy storage in the laser cavity to energy loss per unit time. In passive Q-switched lasers, materials exhibiting saturable absorption effects are employed as saturable absorbers. When a lower light intensity is applied to a saturable absorber, the transmittance of the material undergoes a change in accordance with the intensity, thereby regulating the energy loss within the cavity and resulting in the generation of a Q-switched laser output.[20]The absence of external modulation devices renders the structure more compact and cost-effective, thereby enhancing its suitability for a range of laser application scenarios.

When studying passive Q-switched solid-state lasers, it is necessary to conduct in-depth analysis of the dynamic characteristics of various particles inside the laser. The dynamic characteristics of lasers are mainly reflected in the variation laws of photon number density, inverted particle number density, and the ground state particle number of saturable absorbers. In order to better understand these processes, the energy level transition diagram of a four level system and the energy level diagram of a saturable absorber are often used for description, as shown in Figure 1 below.[21]

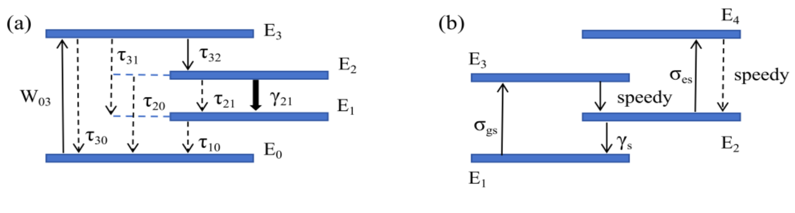

Figure 1: Laser energy level transition diagram (a) and saturable absorber energy level transition diagram (b).

Figure 1(a) illustrates that initially, all atoms in the laser are at the lowest energy level, E_0. Upon radiation excitation of the laser source, particles undergo a transition from E_0 to the broadband excited state, E_3. As E_3 is a broadband energy level, the majority of particles will rapidly transition to the narrower energy level, E_2, through non-radiative transitions. In a four-level system, laser transitions occur between the upper and lower energy levels, E_2 and E_1, of the laser. The transition of particles from the E2 to the E1 state is accompanied by the emission of a laser beam, with the particles subsequently returning to the ground state E_0 via a rapid non-radiative transition. This process description elucidates the role of a four-level system in lasers and provides a comprehensive analysis of the transition process of particles between energy levels. Figure (b) illustrates the energy level transition diagram of a saturable absorber, wherein σ_{gs} represents the ground state absorption cross-section and σ_{es} represents the excited state absorption cross-section. When a saturable absorber is subjected to laser action, particles undergo a transition from the ground state energy level E1 to a higher energy level E3. In an ideal scenario, where the material is an excellent saturable absorber, the value of σ_{gs} should be greater than σ_{es}. Following excitation, particles will then transition to a higher energy level E4. As the number of particles is depleted, the ground state absorption in the laser resonant cavity increases, leading to an increase in residual losses.

Based on the four level transition system, the study will start from the four level rate equation, use Nd^{3+}: YAG as the gain medium, and use the parameters of graphene as the input parameters of the saturable absorber to construct the following rate equation:

$$\frac{d\varphi}{dt} = \frac{\varphi}{t_r}[2\sigma nL - 2\sigma_{gs}n_{gs}l_s - 2\sigma_{es}(n_{0s} - n_{gs})l_s - (\ln\frac{1}{R} + \delta)] \tag{1}$$

$$\frac{dn}{dt} = w_p(1 - \frac{n}{N_T}) - \gamma\sigma c\varphi n - \frac{n}{\tau_a} \tag{2}$$

$$\frac{dn_{gs}}{dt} = \frac{(n_{0s} - n_{gs})}{\tau_{gs}} - \tau_{gs}c\varphi n_{gs} \tag{3}$$

Among them, φ represents the photon number density inside the laser cavity; t_r is the round-trip time of photons in the laser cavity, and l_c is the length of the resonant cavity's light passage; σ is the stimulated emission cross-section of the gain medium (Nd: YAG); n is the inverse particle number density; L represents the length of the gain medium; σ_{gs} is the ground state absorption cross section of a saturable absorber (graphene); n_{gs} is the ground state particle number density; l_s is the light transmission length of the saturable absorber; σ_{es} is the excited state absorption cross section of a saturable absorber; n_{0s} is the overall particle number density of the saturable absorber; R is the reflectivity of the output mirror; δ represents the dissipative loss of photons inside the laser cavity; w_p represents the laser pumping rate; N_T is the total particle number density of the laser gain medium; γ represents the inversion factor of a four level system; c is the speed of light; τ_a is the high-energy lifetime of the gain medium; τ_{gs} is the recovery time of the saturable absorber; In order to achieve simulation, the following simulation parameter Table 1 is introduced by referring to various literature and experimental conditions.[22-25]

Table 1: Simulation parameter table

Simulation parameters	Meaning/Unit	Numerical value
σ	Nd:YAG stimulated emission cross-section/ m^{-2}	5.4×10^{-23}
l_c	The optical length of the resonant cavity/m	0.001
σ_{gs}	Ground state absorption cross-section of graphene/m^{-2}	8×10^{-18}
Simulation parameters	Meaning/Unit	Numerical value
l_s	The crystal length/m	0.001
σ_{es}	Excited state absorption cross section of graphene/m^{-2}	2×10^{-18}
R	Mirror reflectivity/%	0.7
N_T	Nd:YAG total particle number density/m^{-3}	1.68×10^{26}
c	Speed of light/$(m \cdot s^{-1})$	3×10^{8}
τ_a	High energy lifetime of gain medium/s	7.5×10^{-4}
τ_{gs}	Graphene recovery time/s	3×10^{-9}

ISSN 2706-655X Vol.6, Issue 6: 8-17, DOI: 10.25236/IJFET.2024.060602

3. Result Analysis.

Once the parameters of the laser and saturable absorber have been established, the pump rate (w_p) of the laser source should be set to $1.6\times10^{28}s^{-1}$, the cavity loss (δ) of the laser to 0.02, and the simulation time range to 0.05 seconds. The resulting numerical simulation, conducted using MATLAB, is presented in the subsequent Figure 2.

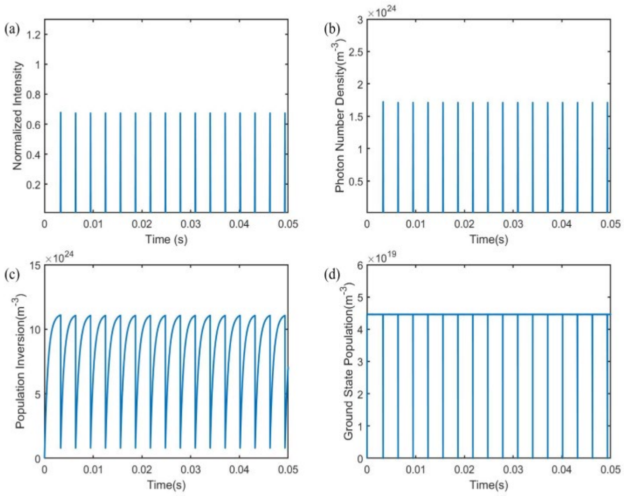

Figure 2: (a) Passive Q-switching pulse sequence, (b) Photon number density, (c) Reverse the number of particles, (d) Number of ground state particles.

As illustrated in Figure 2(a), the fabricated passive Q-switched laser exhibits stable pulse output, thereby confirming the laser's stability under specified parameters. Figures (b), (c), and (d) illustrate the dynamic alterations in photon number density, the number of inverted particles, and the number of saturable absorber ground state particles, respectively, at a constant pump rate. Prior to the arrival of the light pulse, the number of inverted particles within the laser cavity experiences a rapid accumulation until the condition for which the right-hand side of the photon number density differential equation in the four-level system is greater than zero is met. At this juncture, the number of inverted particles commences a rapid decline, while the photon number density experiences a rapid increase and attains its peak value. As the photon number density increases, the number of inverted particles and the number of saturable absorber ground state particles decrease further, forming a complete pulse process of laser output. On this basis, the pump source rate and cavity dissipation loss parameters of the laser were adjusted separately while the saturable absorber and other system parameters remained unchanged. This allowed the influence of different parameters on the output performance of passive Q-switched lasers to be studied.

3.1. The Influence of Pump Rate on Passive Q-switching Output Results.

In order to study the effect of different laser source pump rates w_p on passive Q-switched lasers, it is necessary to maintain constant not only other system parameters but also the loss of laser cavity dissipation. The pump rates (w_p) are adjusted to $1.6\times10^{28}s^{-1}$, $1.8\times10^{28}s^{-1}$, $2.0\times10^{28}s^{-1}$, and $2.2\times10^{28}s^{-1}$, in ascending order. As illustrated in Figure 3, the numerical simulation demonstrates that the pulse sequence undergoes a transformation. While the pulse sequence maintains a stable Q-switched output with increasing pump rates, the number of pulses gradually increases within a fixed simulation time (0.05 seconds), resulting in shorter pulse intervals. The pulse widths at pump rates of $1.6\times10^{28}s^{-1}$, $1.8\times10^{28}s^{-1}$, $2.0\times10^{28}s^{-1}$, and $2.2\times10^{28}s^{-1}$ were calculated to be 670 ps, 516 ps, 447 ps, and 406 ps, respectively.

Figure 4 provides further insight into the relationship between pulse width and pump rate. As the pump rate rises from 1.6 to 2.2, the pulse width declines from the pulse sequence of 670 ps to 406 ps, and the decreasing trend gradually diminishes. The increase in pulse width can be attributed to the accumulation of particle reversals in the laser cavity, which occurs at a faster rate as the pump rate rises. This results in a shorter interval between pulses and an elevated repetition frequency. Furthermore, an increase in the pumping rate typically results in a reduction in pulse width. The higher pumping rate facilitates a greater energy accumulation rate within the laser cavity, leading to a shorter release time and the generation of pulses with a higher degree of sharpness and narrowness.

ISSN 2706-655X Vol.6, Issue 6: 8-17, DOI: 10.25236/IJFET.2024.060602

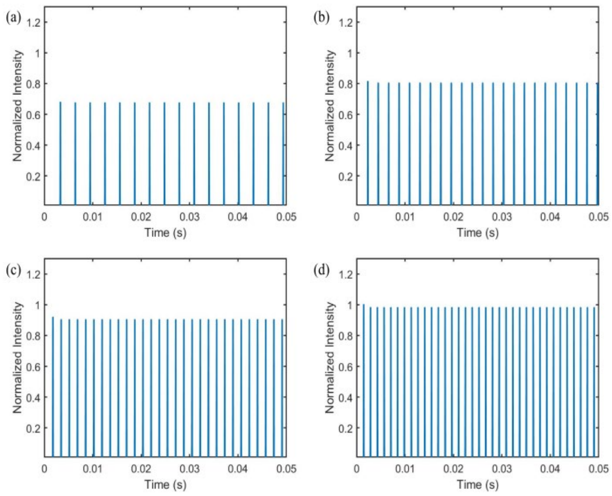

Figure 3: Pulse sequence diagram at different pumping rates(a)1.6×10^{28}s^{-1},(b)1.8×10^{28}s^{-1}, (c)2.0×10^{28}s^{-1}, (d)2.2×10^{28}s^{-1}.

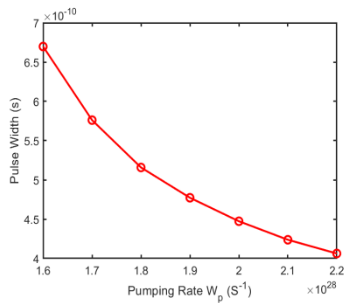

Figure 4: Trend of pulse width variation with pump rate.

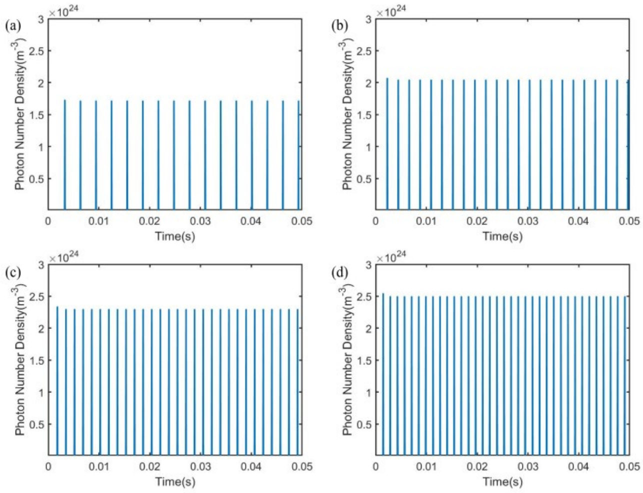

Figure 5: Photon number density plot at different pumping rates (a)1.6×10^{28}s^{-1},(b)1.8×10^{28}s^{-1}, (c)2.0×10^{28}s^{-1}, (d)2.2×10^{28}s^{-1}.

In order to gain further insight into the effect of gradually increasing the pumping rate of the laser source on the output of Q-switched lasers, the evolution paths of photon number density, inverted particle number density, and ground state particle number density were numerically simulated. As illustrated in Figure 5, an increase in the pumping rate from $1.6\times10^{28}s^{-1}$ to $2.2\times10^{28}s^{-1}$ results in a corresponding rise in the photon number density, which increases from $1.75\times10^{24}m^{-3}$ to $2.5\times10^{24}m^{-3}$. Additionally, the photon number density pattern exhibits a notable densification, akin to a pulse sequence.

ISSN 2706-655X Vol.6, Issue 6: 8-17, DOI: 10.25236/IJFET.2024.060602

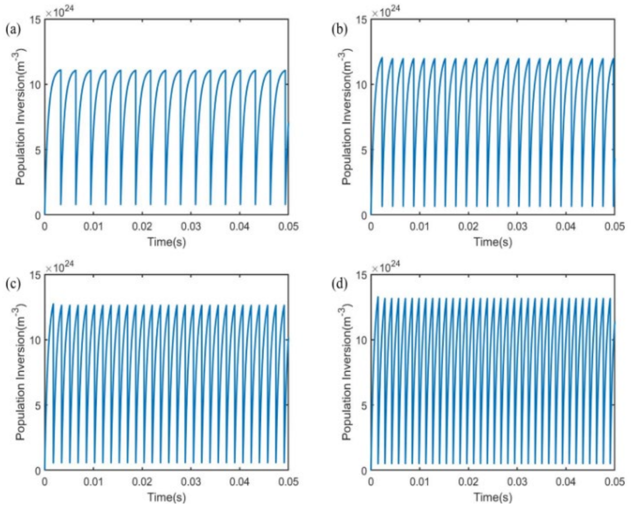

Figure 6: Reverse particle number density at different pumping rates (a) 1.6×10^{28}s^{-1},(b)1.8×10^{28}s^{-1}, (c)2.0×10^{28}s^{-1}, (d)2.2×10^{28}s^{-1}.

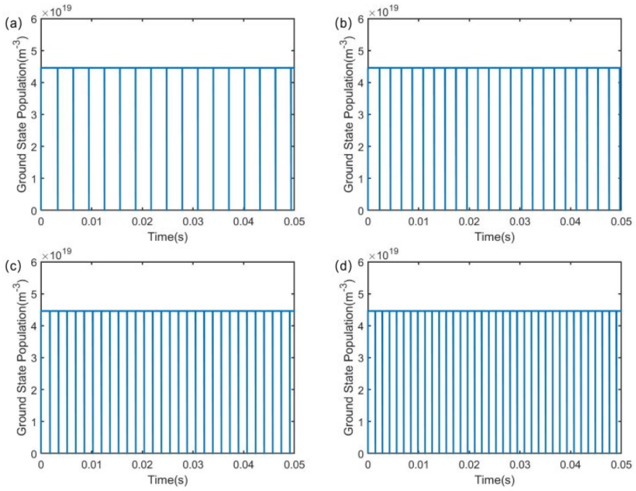

Figure 7: Ground state particle number density at different pumping rates (a) 1.6×10^{28}s^{-1},(b)1.8×10^{28}s^{-1}, (c)2.0×10^{28}s^{-1}, (d)2.2×10^{28}s^{-1}.

The numerical simulations of the number density of inverted particles and ground state particles, as illustrated in Figures 6 and 7, demonstrate that as the pumping rate increases, both the number density of inverted particles and ground state particles exhibit a tendency towards greater density. At higher pump rates, particles within the laser reach higher energy levels with greater rapidity through excitation transitions. Consequently, a greater number of particles will transition to the upper energy level of the laser in a shorter time. This directly results in an increase in the accumulation rate of reversed particle numbers, which in turn leads to an increase in the density of reversed particle numbers. Meanwhile, as the ground state particles are continuously excited to the excited state, the peak of the number of inverted particles will also correspondingly increase. As the pumping rate increases, the changes in the number density of inverted particles and ground state particles in the system become more frequent and concentrated. This phenomenon can be attributed to the acceleration of energy accumulation and release rates within the laser cavity, which is a consequence of the increase in pumping rate. In summary, an elevated pumping rate facilitates the accelerated dynamic transitions of particles between high energy levels and ground states, leading to an augmented peak number of inverted particles and a more condensed periodic variation. This phenomenon elucidates the correlation between the dynamic behaviour within the laser and the pumping rate, which is of paramount importance for optimising the pulse output characteristics of passive Q-switched lasers.

3.2. The Influence of Laser Cavity Loss on Passive Q-switching Output Results.

In addition to the pumping rate of the laser, the dissipative losses inside the cavity represent a significant factor affecting the output performance of passive Q-switched solid-state lasers based on graphene. In order to investigate the impact of dissipative losses on the output performance of the laser, this study gradually increased the dissipative losses from 0.02, 0.08, 0.14, and 0.20 under the condition of maintaining a constant pump rate. The corresponding dissipative losses were calculated using a numerical simulation pulse sequence, the results of which are shown in Figure 8. The pulse widths were found to be 410ps, 787ps, 970ps, and 1.4ns.

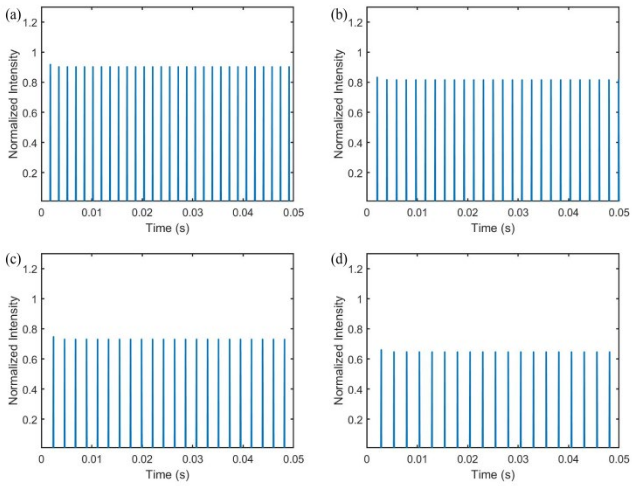

Figure 8: Pulse sequence diagram under different dissipative losses (a)0.02,(b)0.08, (c)0.14, (d)0.20.

Further calculation of the pulse width yielded the result displayed in Figure 9. It is evident that, contrary to the result of increasing the pump rate, which leads to a denser pulse sequence, the pulse width sharply increases as the dissipative loss increases. This phenomenon can be attributed to the fact that as the internal energy loss of the laser intensifies, the photon number density in the system is unable to accumulate sufficient energy at a sufficient rate to meet the energy release threshold under Q-switching conditions. This, in turn, affects the frequency of pulse generation. Dissipative loss represents the energy loss occurring within the laser cavity. As the loss increases, the number of photons travelling back and forth within the cavity decreases, resulting in a slower accumulation rate of photon number density. Concurrently, the decrease in the number of inverted particles also slows down, and the system takes longer to reach the conditions for triggering pulse output. Consequently, the generation of pulses becomes sparser and the output frequency decreases.

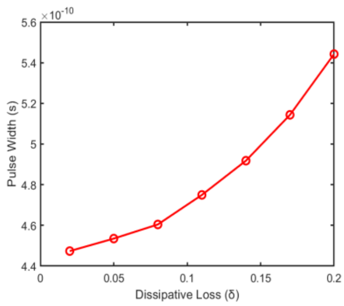

Figure 9: Trend of pulse width variation with dissipative loss.

The utilisation of numerical simulations of photon number density, inverted particle number density, and ground state particle number density enables a more accurate revelation of the impact of changes in dissipative loss δ on passive Q-switched solid-state lasers. As illustrated in Figure 10, an increase in dissipative loss from 0.02 to 0.20 results in a corresponding decline in photon number density, from 2.25×10^{24} to 1.64×10^{24}. This is due to the fact that dissipative loss has a direct impact on the accumulation and release of energy within the laser cavity. An increase in loss results in a greater loss of energy during each round trip of the laser cavity, which in turn leads to a reduction in the rate of accumulation of photon number density.

ISSN 2706-655X Vol.6, Issue 6: 8-17, DOI: 10.25236/IJFET.2024.060602

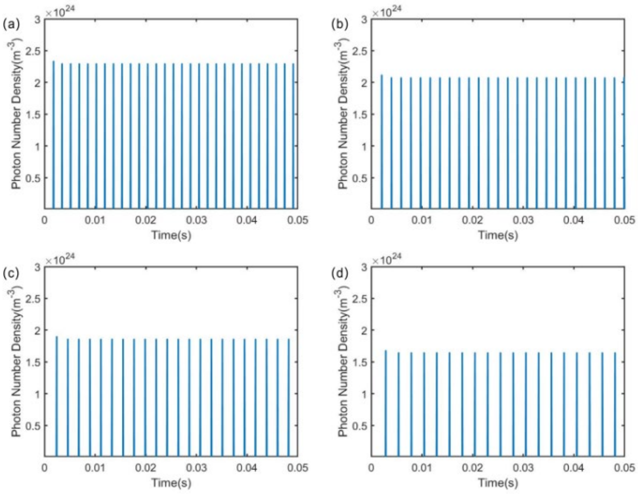

Figure 10: Photon number density under different dissipative losses (a)0.02,(b)0.08, (c)0.14, (d)0.20.

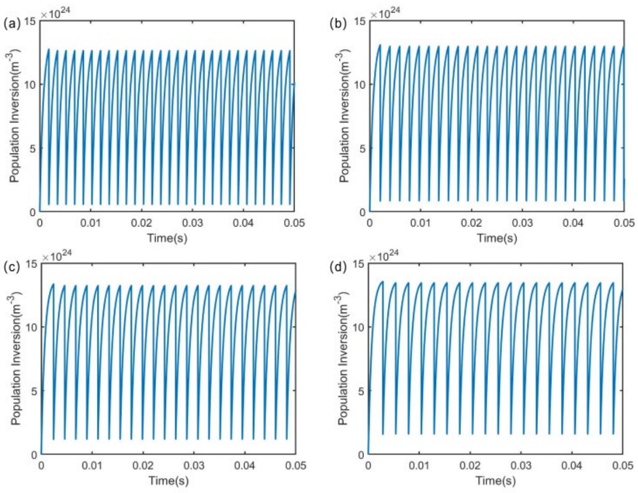

Figure 11: Reverse particle number density under different dissipative losses (a)0.02,(b)0.08, (c)0.14, (d)0.20.

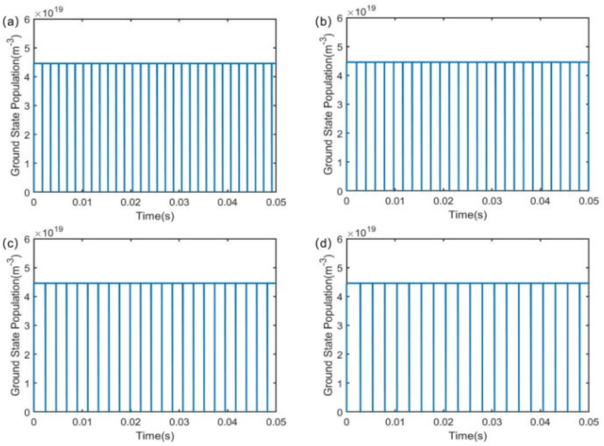

Figure 12: Ground state particle number density under different dissipative losses (a)0.02,(b)0.08, (c)0.14, (d)0.20.

Through numerical simulations of the number of inverted particles and ground state particles, Figures 11 and 12 show the results under different dissipation loss conditions. When the dissipation loss increases, although the peak values of the number of inverted particles and ground state particles remain unchanged, the time for the system to reach sufficient photon density is prolonged, resulting in an increase in the time interval between pulses and a sparser pulse sequence. At higher dissipation losses, the laser gain is mainly limited by the pumping rate, and the number of inverted particles tends to saturate at higher pumping rates. This indicates that even with an increase in losses, the number of inverted particles can still reach saturation within each pulse cycle, so its peak remains unchanged. Similarly, the ground state particle number density of saturable absorbers tends to saturate, and its dynamic changes are mainly influenced by light intensity. However, due to the increase in intracavity losses, the system requires more time to accumulate sufficient photon number density, thereby prolonging the triggering time of each pulse and resulting in a longer period of the pulse sequence.

4. Conclusions

This article employs Nd^{3+}: YAG as the gain medium and graphene parameters as the input parameters for the saturable absorber. Based on the four-level passive Q-switching rate equation, numerical simulations were conducted using the fourth-order Runge-Kutta method in Matlab with the objective of achieving stable Q-switching pulse output. Further analysis was conducted to investigate the impact of alterations in system parameters, including the laser source pumping rate and cavity dissipation losses, on the dynamic behaviour of Q-switched pulse sequences, as well as on the photon number density, inverted particle number density and ground state particle number density. The results of the analysis demonstrate that modifying the pumping rate of the laser source and the cavity dissipation loss can effectively regulate the triggering time and frequency of passive Q-switched solid-state lasers utilising graphene as a saturable absorber. Consequently, alterations to these parameters will markedly influence the accumulation rate of photon number density, inverted particle number density, and ground state particle number density, consequently affecting the dynamic evolution characteristics of laser output. The research results provide a crucial theoretical foundation for regulating the output characteristics of passive Q-switched solid-state lasers.

References

[1] Meier, M., Romano, V., & Feurer, T. (2007). Material processing with pulsed radially and azimuthally polarized laser radiation. Applied Physics A, 86, 329-334.
[2] Vanwiggeren, G. D., & Roy, R. (1998). Communication with chaotic lasers. Science, 279(5354), 1198-1200.
[3] Corkum, P. B., Brunel, F., Sherman, N. K., & Srinivasan-Rao, T. (1988). Thermal response of metals to ultrashort-pulse laser excitation. Physical review letters, 61(25), 2886.
[4] Wei C.J, Yan R.P, Li X.D, Meng X.X, & Liu X.Y (2021). Research progress on sub nanosecond lasers for 3D imaging lidar applications. Optical Precision Engineering (06), 1270-1280
[5] Salem, A., El Harras, M., Ramadan, A., Gamil, H., Abdul Rahman, A., & El-Said, K. (2010). Use of the Q-switched Nd: YAG laser for the treatment of pigmentary disorders in Egyptians. Journal of Cosmetic and Laser Therapy, 12(2), 92-100.
[6] Flegel, L., Kherani, F., & Richer, V. (2022). Review of eye injuries associated with dermatologic laser treatment. Dermatologic Surgery, 48(5), 545-550.
[7] Wagner, A., Lütke, M., Wetzig, A., & Eng, L. M. (2013). Laser remote-fusion cutting with solid-state lasers. Journal of Laser Applications, 25(5).
[8] Song, Y. W., Jang, S. Y., Han, W. S., & Bae, M. K. (2010). Graphene mode-lockers for fiber lasers functioned with evanescent field interaction. Applied Physics Letters, 96(5).
[9] Popa, D., Sun, Z., Hasan, T., Torrisi, F., Wang, F., & Ferrari, A. C. (2011). Graphene Q-switched, tunable fiber laser. Applied Physics Letters, 98(7).
[10] Wu G, Zhang Z, Wang T, Ji L.L, Cui Y, Gao Y.G&Sui Z (2024). LD end pumped Tm: SrF2 electro-optic Q-switched laser. Intense Laser and Particle Beam (06), 52-57
[11] Guo, L., Yang, Y., Wang, R., Zhang, B., Li, T., Zhao, S., ... & Yang, K. (2021). Experimental and theoretical study of an actively Q-switched TM: YLF laser with an acousto-optic modulator. Molecules, 26(23), 7324.
[12] Gao, L., Ding, Y., Zhai, X., Min, H., Liu, G., Lan, R., & Shen, Y. (2024). Passively Q-switched 2 μm laser based on graphene/BN heterostructure as saturable absorber. Optics & Laser Technology, 168, 109852.
[13] Zhao, J., Yang, X., Liu, Y., Jin, L., Yu, R., Zhou, X., & Cheng, P. (2024). Passively Q-switched 2.3 μm Tm: YVO 4 laser using a Cr: ZnS saturable absorber. Optics Letters, 49(4), 862-865.
[14] Dong, J., Shirakawa, A., & Ueda, K. I. (2005). Numerical simulation of a diode-laser-pumped self-Q-switched Cr, Yb: YAG microchip laser. Optical review, 12, 170-178.

ISSN 2706-655X Vol.6, Issue 6: 8-17, DOI: 10.25236/IJFET.2024.060602

[15] Yu-Ye, W., De-Gang, X., Jing-Ping, X., Zhuo, W., Peng, W., & Jian-Quan, Y. (2008). Numerical modelling of QCW-pumped passively Q-switched Nd: YAG lasers with Cr4+: YAG as saturable absorber. Chinese Physics Letters, 25(8), 2880.

[16] Aubourg, A., Didierjean, J., Aubry, N., Balembois, F., & Georges, P. (2013). Passively Q-switched diode-pumped Er: YAG solid-state laser. Optics letters, 38(6), 938.

[17] Lin, Y. Y., Lee, P., Xu, J. L., Wu, C. L., Chou, C. M., Tu, C. Y., ... & Lee, C. K. (2016). High-pulse-energy topological insulator Bi 2 Te 3-based passive Q-switched solid-state laser. IEEE Photonics Journal, 8(4), 1-10.

[18] Li, L., Cui, W., Yang, X., Zhou, L., Yang, Y., Xie, W., ... & Han, J. (2020). A high-beam-quality passively Q-switched 2 μm solid-state laser with a WSe2 saturable absorber. Optics & Laser Technology, 125, 105960.

[19] Du, Y., Yao, B., Duan, X., Cui, Z., Ding, Y., Ju, Y., & Shen, Z. (2013). Cr: ZnS saturable absorber passively Q-switched Tm, Ho: GdVO 4 laser. Optics Express, 21(22), 26506-26512.

[20] Zayhowski, J. J., & Kelley, P. L. (1991). Optimization of Q-switched lasers. IEEE journal of quantum electronics, 27(9), 2220-2225.

[21] Koechner, W. (2013). Solid-state laser engineering (Vol. 1). Springer.

[22] Tang, D. Y., Ng, S. P., Qin, L. J., & Meng, X. L. (2003). Deterministic chaos in a diode-pumped Nd: YAG laser passively Q switched by a Cr 4+: YAG crystal. Optics letters, 28(5), 325-327.

[23] Yang, Y., Kolesov, G., Kocia, L., & Heller, E. J. (2017). Reassessing graphene absorption and emission spectroscopy. Nano letters, 17(10), 6077-6082.

[24] Xing, G., Guo, H., Zhang, X., Sum, T. C., & Huan, C. H. A. (2010). The physics of ultrafast saturable absorption in graphene. Optics express, 18(5), 4564-4573.

[25] Hwang, E. H., & Das Sarma, S. (2008). Single-particle relaxation time versus transport scattering time in a two-dimensional graphene layer. Physical Review B—Condensed Matter and Materials Physics, 77(19), 195412.